Accepted Manuscript

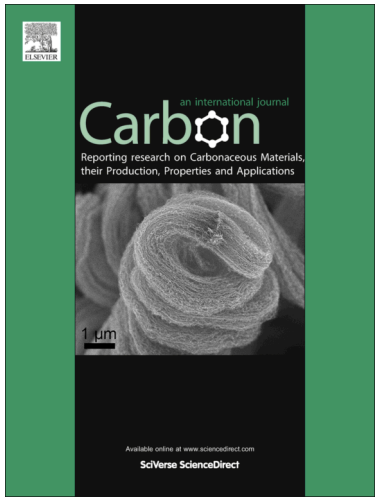

Activation of a spherical carbon for toluene adsorption at low concentration

A.J. Romero-Anaya, M.A. Lillo-Ródenas, A. Linares-Solano

PII: S0008-6223(14)00520-X
DOI: http://dx.doi.org/10.1016/j.carbon.2014.05.066
Reference: CARBON 9032

To appear in: *Carbon*

Received Date: 20 March 2014
Accepted Date: 23 May 2014

Please cite this article as: Romero-Anaya, A.J., Lillo-Ródenas, M.A., Linares-Solano, A., Activation of a spherical carbon for toluene adsorption at low concentration, *Carbon* (2014), doi: http://dx.doi.org/10.1016/j.carbon.2014.05.066

Activation of a spherical carbon for toluene adsorption at low concentration

A.J. Romero-Anaya, M.A. Lillo-Ródenas*, A. Linares-Solano

Departamento de Química Inorgánica, Universidad de Alicante, Ap. Correos 99. E-03080, Alicante, Spain. Phone number: +34 965909350; Fax number +34 965903454; E-mail: mlillo@ua.es

Abstract

This paper complements a previous one [1] about toluene adsorption on a commercial spherical activated carbon and on samples obtained from it by CO_2 or steam activation. The present paper deals with the activation of a commercial spherical carbon (SC) having low porosity and high bed density (0.85 g/cm^3) using the same procedure. Our results show that SC can be well activated with CO_2 or steam. The increase in the burn-off percentage leads to an increase in the gravimetric adsorption capacity (more intensively for CO_2) and a decrease in bed density (more intensively for CO_2). However, for similar porosity developments similar bed densities are achieved for CO_2 and steam. Especial attention is paid to differences between both activating agents, comparing samples having similar or different activation rates, showing that CO_2 generates more narrow porosity and penetrates more inside the spherical particles than steam. Steam activates more from the outside to the interior of the spheres and hence produces larger spheres size reductions. With both activation agents and with a suitable combination of porosity development and bed density, quite high volumetric adsorption values of toluene (up to 236 g toluene/L) can be obtained even using a low toluene concentration (200 ppmv).

1. Introduction

Volatile organic compounds (VOCs) are emitted as gases from different sources and they have harmful effects on the environment [2,3]. Furthermore, they cause alterations in the nervous system and are a source of risk for cancer [4] and mutations at the genetic level [5]. Generally, VOCs are produced in gas phase and at low concentrations [6,7]. Hence, nowadays new technologies with high efficiencies that seek to optimize the various existing methods for controlling VOC emissions have been implanted [8].

Among all these techniques [9-13], adsorption is one of the most effective methods and presents a great range of applicability in terms of concentrations and flow rates. As an example, it can be used for adsorption of gases at low concentrations with low operation costs employing activated carbons (ACs) as adsorbents [6,7]. Activated carbons are the most often used materials for this purpose due to their hydrophobicity and high specific surface areas [14-16].

The morphology of the activated carbons is very important for their final applications. For example, when ACs are used in fixed beds, spherical activated carbons (SACs) have advantages over granular activated carbons due to better packaging and lower pressure drop. Besides, an spherical activated carbon has other characteristics which stand still more its potential advantages, such as high wear resistance, high mechanical strength, good adsorption performance, high purity, low ash content,

smooth surface, good fluidity, high micropore volume and more controllable pore size distribution [17,18]. All these advantages have allowed SACs to be used in several applications, both in gas phase [1] and in solution [19-25].

These advantages make that SACs are being recently prepared from several methods and precursors. Thus, using polymerization methods, different precursors such as aerogels [22], divinylbenzene-derived polymers [23] or urea/formaldehyde resin [24] have been used. Using agglomeration methods, different bituminous coals have led to the preparation of spherical carbons [25]. Also, spherical activated carbons have been prepared from mixtures of resin and activated carbon [26] and, recently, hydrothermal treatment of different lignocellulosic materials [27-29] or carbohydrates [30-33] has been used.

In a previous paper [1] we selected a commercial spherical activated carbon supplied by Kureha Corporation (KC) having a surface area of 1291 m^2/g and a bed density of 0.59 g/cm^3 and we analyzed its further activation and the results were analyzed on gravimetric and volumetric terms. [1]. The resulting samples were used in toluene adsorption at low concentration (200 ppmv in air) [1]. As expected, the porosity and surface area increased with the burn-off percentage, but the bed density decreased. The highest toluene volumetric adsorption capacity (230 g toluene/L) was obtained for the starting sample, which had the highest bed density (0.59 g/cm^3), and not for the sample having the highest porosity (2600 m^2/g), for which its bed density was only 0.31 cm^3/g.

According to these results, the present work analyzes a different precursor; a dense spherical carbonized material (hereafter GE), with the purpose of obtaining samples combining high porosities and high bed densities.

Two series of SACs have been prepared by physical activation of GE, one with CO_2 and one with steam. SAC samples having similar burn-off percentages (obtained using both a similar and a different activation rate) are compared to deepen into the differences induced by both activating agents. Some of these SACs have been applied to the adsorption of toluene at low concentration, analysing the results on a gravimetric and volumetric basis.

Additionally, and for comparison purposes, two high quality commercial samples are used as references; a spherical activated carbon from Gun-ei Industry, referred to as ACGE, and a well performing commercial activated carbon for evaporative emission control from MeadWestvaco, referred to as WVA1100 which also was used as reference in previous toluene adsorption studies [1,10,15,16,43].

2. Materials and methods

2.1. Materials

A commercial spherical carbon obtained from a phenolic resin by the process described in the Japanese Patent Publication (Kokoku) No. 62-11611 and supplied by Gun-Ei Chemical Industry (Headquarters: Takasaki-shi, Gunma Japan) has been used as the spherical carbon precursor of two series of SACs prepared by either CO_2 or steam activation.

The two additional commercial samples used are a commercial spherical activated carbon (ACGE, also supplied Gun-Ei Chemical Industry) and a granular activated carbon (WVA1100 10 x 25 mesh, supplied by Mead Westvaco).

2.2. Methods

2.2.1. Activation procedure

SACs were prepared from GE by physical activation using CO_2 or steam. For CO_2, a horizontal quartz fixed bed reactor 2 m long and 0.07 m diameter was used and the precursor to be activated was placed in a flat crucible. A precursor weight of 2 g, a flow of 80 mL/min of CO_2, a temperature of 880 ºC and times of activation of 10, 15, 24 and 30 hours were used. For steam activation, a vertical quartz reactor with upward flow was employed using a steam flow of 0.9 L/min, a precursor weight of 2 g, a final temperature of 840 ºC and activation times of 0.75, 2.0, 3.5, and 4 hours. At these flow rates, fluidisation of the bed takes place [32]. Under these experimental conditions samples having comparable burn-off percentages have been obtained from both activating agents but their activation rates are different.

To obtain with both activating agents SAC samples at similar activation rate, that is having similar burn-off percentages in a given activation time, e.g., about 3h, the temperature of the CO_2 activation has been increased from 880ºC to 970 ºC. The nomenclature of the different spherical activated carbons derived from GE can be described as follows. Firstly, the precursor (GE) is indicated, secondly the BO percentage and, finally, the type of activating agent used (C for CO_2 and S for steam).

2.2.2. Samples morphologies and bed densities

Morphology of the original GE and of the SACs prepared from it has been studied using Scanning Electron Microscopy (SEM). Bed density (ρ_b; bulk or tap) was measured using an experimental procedure similar to that described by the D2854-89 ASTM method (American Society for Testing and Materials). In our case, the density measurement was performed with 0.5 g of sample using a 10 ml measuring cylinder.

2.2.3. Porosity characterization

The textural characterization of the samples was performed using N_2 adsorption at -196 ºC [34] and CO_2 at 0 ºC [35] in a volumetric Autosorb-6B apparatus from Quantachrome. Before analysis, the samples were outgassed at 250 °C for 4 hours. The BET equation was applied to the nitrogen adsorption data to get the apparent BET surface area (S_{BET}) [36]. The Dubinin-Radushkevich equation was applied to the nitrogen adsorption data to determine the total micropore volume (pores with size <2 nm) and to the carbon dioxide adsorption isotherms to determine narrow micropore volumes (pores with size <0.7 nm) [37]. Pore size distributions were obtained applying the non-local density functional theory (NLDFT) to the N_2 adsorption data at -196 ºC using the software provided by Quantachrome [38].

2.2.4. Oxygen surface characterization

The oxygen surface chemistry of all the samples was analyzed by means of temperature-programmed desorption experiments carried out in a DSC-TGA equipment (TA, SDT 2960 Simultaneous) coupled to a mass spectrometer (Balzers, OmniStar). In

these experiments, 10 mg of sample were heated up to 950 ºC (heating rate 20 ºC/min) under a helium flow rate of 100 mL/min [39].

2.2.5. Adsorption of toluene

The starting material, five selected SACs derived from it and the two commercial samples have been tested for toluene adsorption in a reactor (6 mm inner diameter) coupled to a mass spectrometer (Balzers, OmniStar). The weight of adsorbent was around 0.25 g and a flow of 90 ml/min with a toluene concentration of 200 ppmv was used. Such toluene concentration was generated by bubbling air through a saturator containing toluene placed in a thermostatized bath at -24 ºC, and diluting it with a suitable air flow rate. Concentration was checked using calibrated cylinders provided by Carburos Metálicos S.A. with 200 ppmv toluene in helium and comparing the concentration of the prepared toluene air stream by mass spectrometry. The adsorption temperature was 25 ºC. Before adsorption, the AC samples were outgassed in helium at 250 ºC for 4 h.

Through the graphical representation of the outlet concentration of toluene versus time the corresponding breakthrough curves are obtained. Toluene adsorption capacity was obtained by numerical integration of the breakthrough curves, using the following equation:

$$q_{ads} = \frac{F C_{in}}{m}\left[t_a - \int_{t_a}^{t_b} \frac{C_{out}}{C_{in}} dt\right] \quad (1)$$

Where n_{ads} is the adsorption capacity in mol/g, C_{in} and C_{out} the molar fractions of toluene at reactor inlet and outlet, m is the absorbent weight, t_a the saturation time and F the gaseous molar flow rate. Toluene gravimetric adsorption capacity (g toluene/100 g SAC) was calculated from n_{ads} using toluene molecular weight and expressing the adsorption capacity per 100 grams of adsorbent. Volumetric adsorption capacities (g toluene/L SAC) were calculated considering bed densities of the adsorbents.

3 Results and discussion

3.1. Samples morphologies.

The morphology of the original GE and of the SACs prepared from it with different burn-off percentages has been studied by scanning electron microscopy and particle size distributions have been obtained. As an example, Figure 1 presents the results of the original GE and of two SACs having the same burn-off percentage (65%) and prepared with both activating agents. For most samples particle size distributions were obtained from one microscopy image, although three microscopy images were analysed in sample GE and the obtained particle size distributions agreed very well with the information presented in this paper, obtained using data of one microscopy image.

From it, it can be concluded that: i) the spherical morphology of the starting GE precursor is maintained, ii) the mean particle diameter decreases after activation and iii) steam activation produces a much larger mean particle size reduction than CO_2. Thus, the mean particle size of GE precursor (0.43 mm) decreases to 0.34 mm upon CO_2 activation (sample GE65C; i.e., 21% reduction) and to 0.27 mm upon steam activation (sample GE65S; i.e., 37% reduction). Larger mean size reductions with steam than with

CO_2 were also observed during the activation of the SAC precursor (KC) in our previous publication, although in that case the diameter reductions were lower; 16 % for CO_2 and 27 % for steam, for a 60 % burn-off percentage [1]. Attrition in the steam fluidized bed system can be discarded since there was no particulate carbon found after activation in the experimental system in any of the steam activations performed.

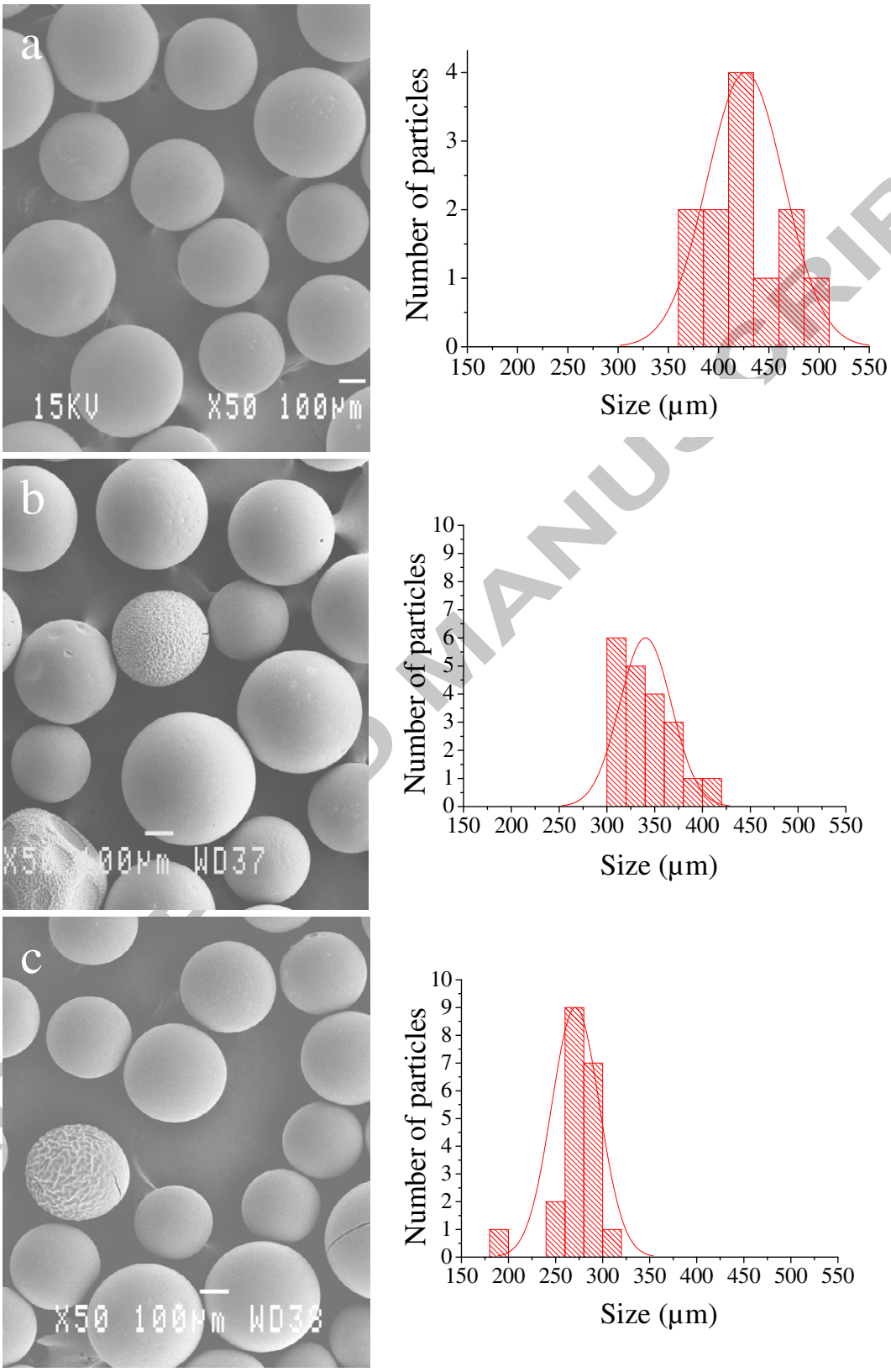

Fig. 1. SEM images and particle size distributions of GE (a), GE65C (b) and GE65S (c).

3.2. Samples characterization

3.2.1. Porous texture

Figure 2a presents the N_2 adsorption-desorption isotherms (at -196 °C) of the prepared samples. From these isotherms it is worth noting: i) the marked microporous character (isotherm type I [40]) of all the SACs obtained from GE, ii) that the changes in the shapes of N_2 adsorption-desorption isotherms with the burn-off percentage of GE are almost limited to the low relative pressure range (<0.2), iii) that the higher the burn-off percentage, the wider the micropore size distribution for the prepared samples and iv) that these series of isotherms clearly show that CO_2 always develops much higher gravimetric adsorption capacity than steam for comparable burn-off percentages.

Table 1 compiles the characteristics of the samples prepared from GE by CO_2 or steam activation and their porous textural characterization; apparent BET surface area, total micropore volume (calculated by nitrogen adsorption) and narrow micropore volume (calculated by carbon dioxide adsorption). Table 1 also includes the textural characterization for commercial samples ACGE and WVA1100. It can be seen that the samples prepared by both activation processes have quite similar degrees of activation, which will allow observing differences caused by both activating agents. It can also be seen that these SACs have been prepared with different activation rates; their temperatures and times of activation are very different (880 ºC and times ranging from 10 to 30 hours for CO_2 activation and 840 ºC and times ranging from 0.75 to 4 hours for steam activation). As expected, in both activation series the burn-off percentage, and hence the activation degree, increases with the activation time.

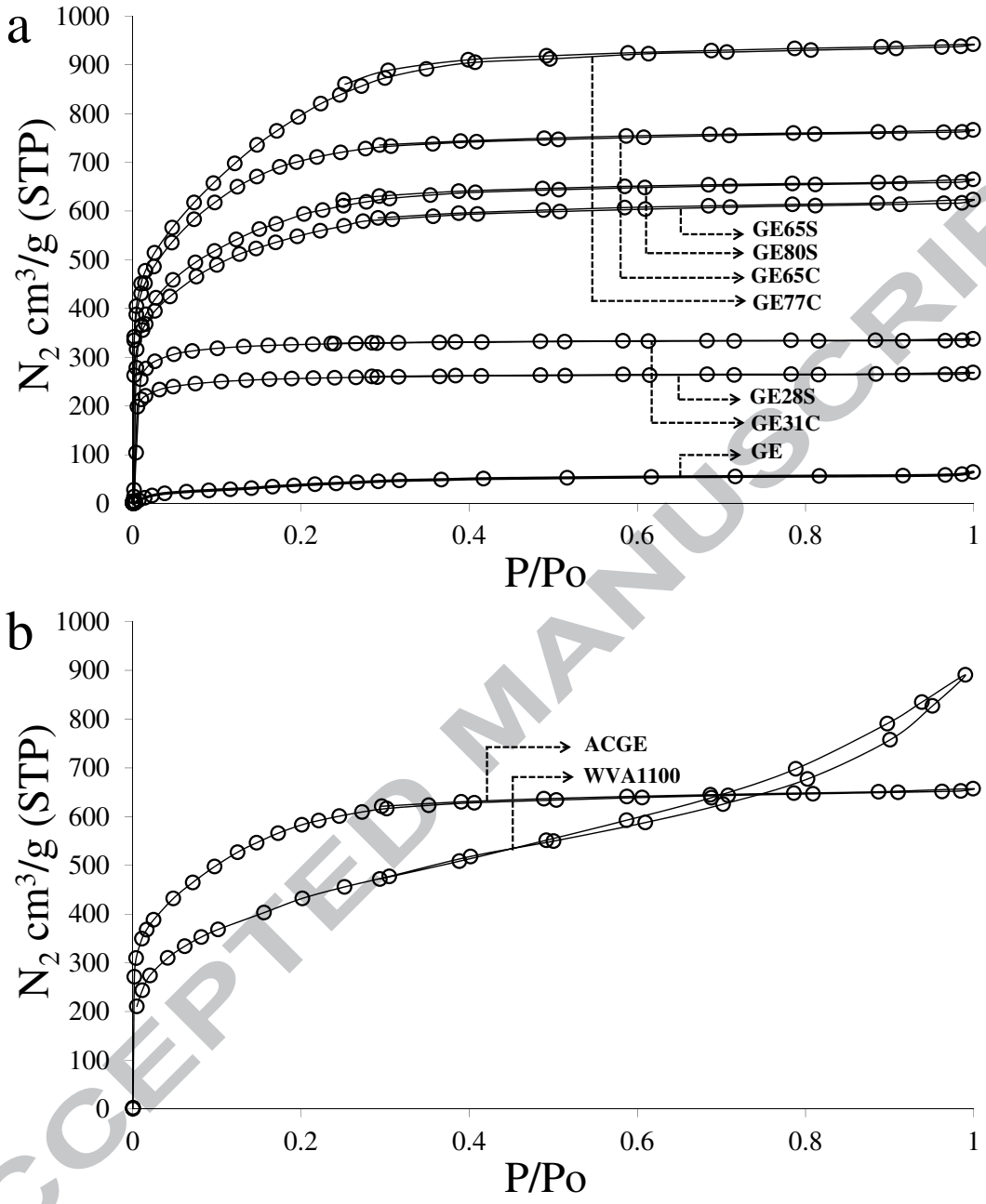

Fig. 2. N_2 adsorption-desorption isotherms at -196 ºC of GE and the SACs prepared from it (a) and of the two commercial samples (b).

From Table 1 also several points merit to be commented: 1) the adsorption capacities (apparent BET surface areas and total micropore volumes) develop

considerably with the burn-off percentage, whereas narrow micropores especially develop at low burn-off percentages; 2) for large BO percentages, much larger porosities are achieved with CO_2 activation than with steam (compare, as an example, samples GE65S and GE65C, with the same burn-off percentage) and 3) the spherical carbon precursor used (GE) can easily be activated with CO_2 or steam allowing to prepare spherical activated carbons with a wide range of adsorption capacities that might reach outstanding values in comparison with published data [41,42]. For example, Baghel et al. obtained spherical activated carbons from polystyrene with BET surface areas ranging between 243 m^2/g and 976 m^2/g (for burn-off percentages between 50 and 66 %) [41]. Tennison also obtained spherical activated carbons from phenolic resin with BET surface areas between 691 m^2/g and 1284 m^2/g [42] and in our previous study, we studied the activation with CO_2 and steam activation of a dense commercial spherical activated carbon (KC) with an apparent surface area around 1300 m^2/g, leading to SACs with surface areas up to 2600 m^2/g [1].

Figure 2b presents the N_2 adsorption isotherms of the two commercial samples used. Sample ACGE has a marked microporous character and high gravimetric adsorption capacity, lower than samples GE65C and GE77C, but similar to sample GE80S. Such similarity seems to indicate that this commercial sample may have been prepared with steam and presumably with a similar burn-off percentage. The commercial sample WVA1100 from MeadWestvaco has a different porosity distribution; in addition to a well-developed microporosity, it presents an important slope at relative pressure higher than 0.2 and a hysteresis cycle, indicative of a well-developed mesoporosity.

Table 1. Summary of the preparation of SACs from GE (experimental conditions and burn-off percentage (BO)), bed densities (ρ_b) and textural characterisation of the SACs and of the two commercial samples.

Sample	Time (h)	Temperature (ºC)	BO (%)	ρ_b (g/cm^3)	S_{BET} (m^2/g)	$V_{DR}N_2$[1] (cm^3/g)	$V_{DR}CO_2$[2] (cm^3/g)
GE	--	--	--	0.85	180	0.07	0.21
GE31C	10	880	31	0.62	1065	0.53	0.47
GE65C	24	880	65	0.39	2426	1.05	0.63
GE77C	30	880	77	0.29	2874	1.12	0.65
GE28S	0.75	840	28	0.69	839	0.41	0.37
GE65S	3.5	840	65	0.49	1891	0.83	0.54
GE80S	4.0	840	80	0.46	2035	0.90	0.60
ACGE	--	--	--	0.45	2060	0.86	0.62
WVA1100	--	--	--	0.29	1757	0.67	0.36

[1]$V_{DR}N_2$ includes pore size <2.0 nm, [2]$V_{DR}CO_2$ includes pore size <0.7 nm.

3.3. Bed densities

Bed density is an important variable for adsorption applications in which the volume occupied by the adsorbent has to be considered. Hence it is important to obtain materials which have, besides good textural properties, high bed densities. Table 1 compiles the bed density of the precursor and the prepared samples and Figure 3a shows the changes observed in the bed density as a function of the burn-off percentage (BO %). As expected bed density decreases with the increase in the burn-off percentage, existing a well-defined relationship between both parameters. It is important to note that: i) the bed densities of these samples are higher than those previously prepared in [1] using other precursor, and ii) depending on the activating agent used the slopes of these relationships are different; larger bed densities are achieved when steam is the activating agent. This can be well observed comparing two samples having similar burn-off percentages (e.g., 65%); samples GE65S and GE65C, for which their bed densities are 0.49 g/cm^3 for steam activation and 0.39 g/cm^3 for CO_2 activation.

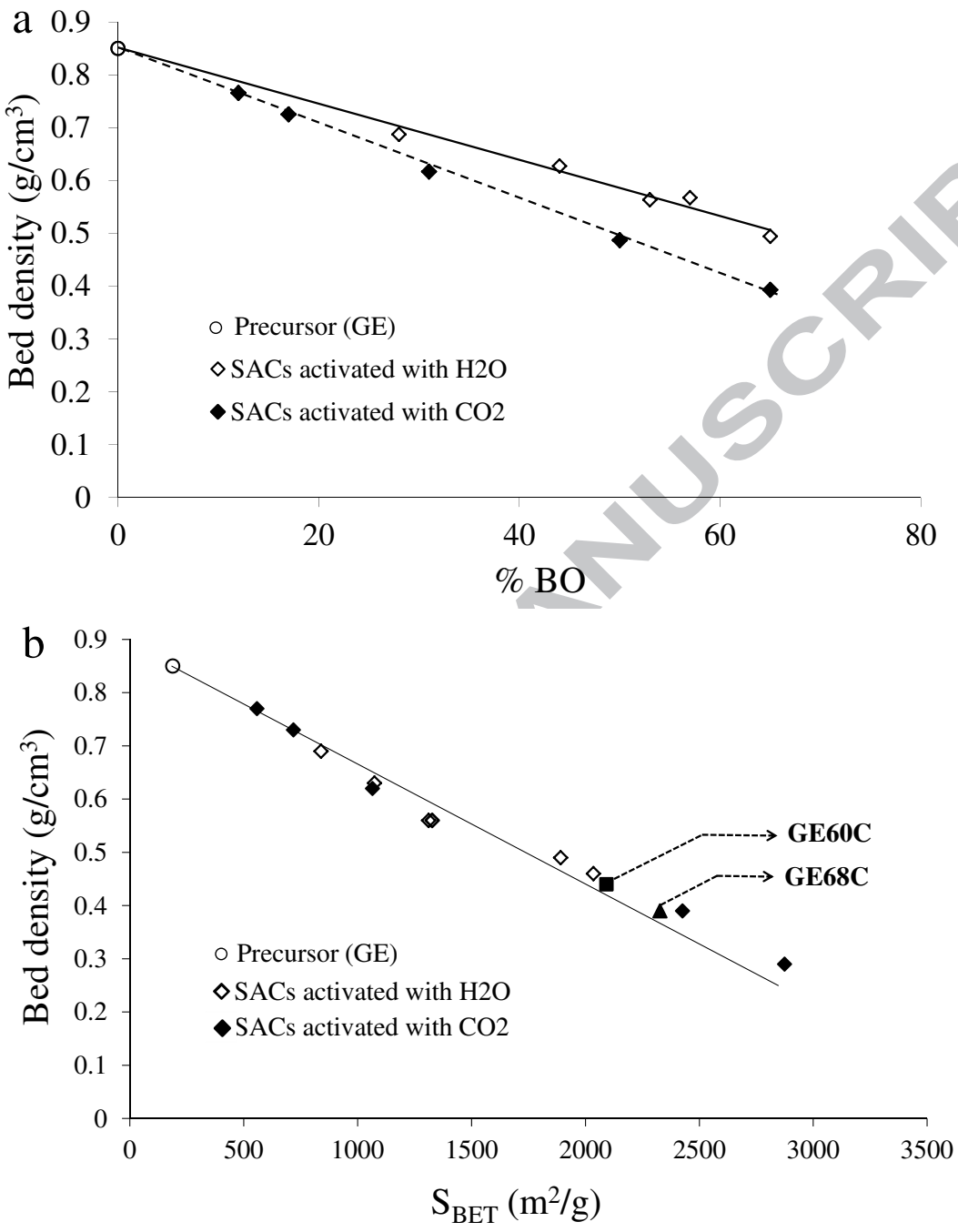

Fig.3. Bed density variation vs burn-off percentage (a) and vs the apparent BET surface area (b). Filled markers are samples activated with CO_2 and empty markers are samples activated with steam. Also, samples activated with CO_2 at 970 ºC and activation times of 3.0 and 3.5 h, samples GE60C and GE68C, are included.

Depending on the activating agent used (CO_2 or steam) the properties of the resulting SACs such as porosity, mean sphere diameter reduction and bed density change in a different manner. In summary, steam, in comparison with CO_2, reduces the sphere diameter more, reduces the bed density less and develops less the sample porosity. All these changes are reasonable considering what has been published before, giving insight and confirming the different ways by which these two activating agents work. In fact, we have observed a similar behaviour during CO_2 and steam activation of a SAC [1] and carbon fibres [43,44]. In both cases these results were analysed and explained according to different activation mechanisms; CO_2 penetrates easier inside the particles, reduces the particle sizes less and develops the porosity more than steam. The fact that steam activation is more focused outside the particles causes more pronounced particle size reduction, lower porosity development and, hence, leads to higher bed density than CO_2, as it has also been observed in this study.

From these results it can be concluded that steam activation presents the advantage of producing SACs with higher bed densities but has the inconvenient, for a comparable burn-off percentage, of developing less porosity than CO_2. To evaluate both parameters simultaneously, Figure 3b presents the changes observed on the bed density as a function of the samples porosities (e.g., apparent BET surface area). A very good correlation is observed, which clearly shows that the advantage of the steam activation of producing samples with higher density is no more evident and it is a consequence of also producing lower porosity development than CO_2 activation. In summary, the activation with CO_2 offers advantages in relation to steam activation since for similar burn-off percentages produces larger porosity developments than steam.

3.4 SACs prepared using the same activation rate

The results of CO_2 and steam activation discussed up to now have been obtained using different activation rates; much higher for steam than for CO_2. To confirm that these observations are not dependent on the different activation rates used, two new CO_2 activated samples have been prepared with a similar activation rate than that used for steam activation. To get it, CO_2 activation was carried out at a temperature of 970 ºC using 3.0 and 3.5 h. These two new samples (GE60C and GE68C) can be compared with two steam activated samples (GE57S and GE65S), that have similar burn-off percentages and have been prepared using the same activation time. Figure 4 shows their N_2 adsorption isotherms and Table 2 their corresponding characterization results.

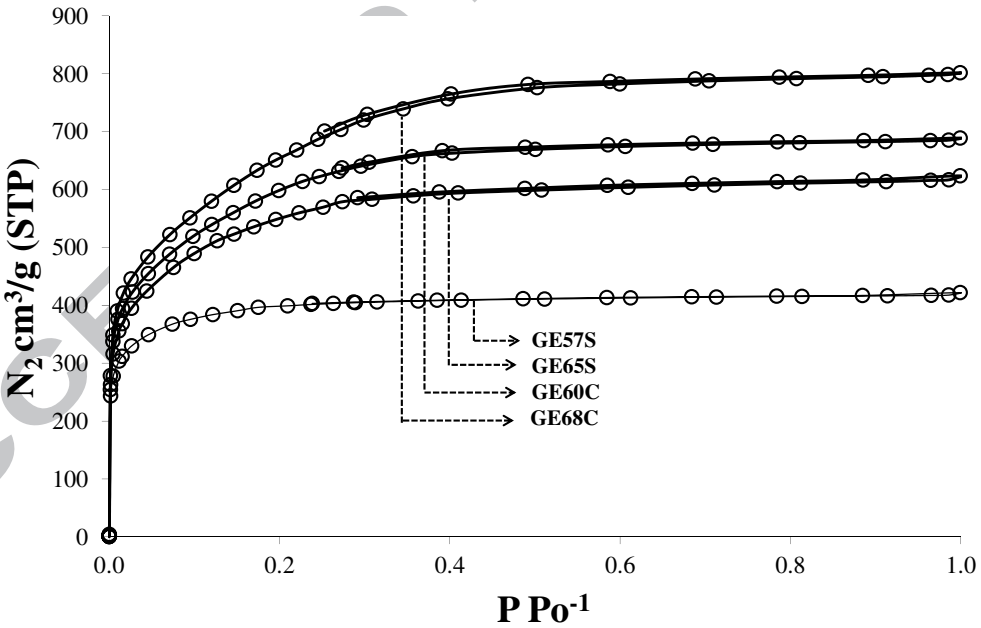

Fig. 4. N_2 adsorption-desorption isotherms at -196 ºC of the SACs prepared with similar activation times, 3.0 and 3.5 h.

Interestingly, Figure 4 and Table 2 confirm that the above conclusions are independent of the activation rate used (i.e., CO_2 develops more porosity than steam and produces lower bed density), as it can also be seen in Fig 3a and b, where these two new CO_2 activated samples are also included.

Table 2. Preparation conditions, bed densities and textural properties of GE65C and GE68C samples.

Sample	Time (h)	Temperature (ºC)	BO (%)	ρ_b (g/cm^3)	S_{BET} (m^2/g)	$V_{DR}N_2$ (cm^3/g)	$V_{DR}CO_2$ (cm^3/g)
GE60C	3.0	970	60	0.44	2092	0.85	0.56
GE57S	3.0	840	57	0.56	1327	0.63	0.48
GE68C	3.5	970	68	0.39	2327	0.96	0.60
GE65S	3.5	840	65	0.49	1891	0.83	0.54

From a comparative analysis of samples GE65C and GE68C, both activated with CO_2, the former using a low activation rate (24 h activation time) and the latter a high activation rate (3.5 h activation time) it can be deduced that both present the same properties independently of the activation rate used. However, a closer look to the knee of the isotherms of these two samples at relative pressures lower than 0.3 (Fig. 3 for GE65C and Fig. 4 for GE68C) permits to conclude that the use of a lower activation rate (24 h activation time) produces a narrower pore size distribution than when using a higher activation rate (3.5 h activation time). That is, a faster activation rate widens the isotherm knee and leads to a wider pore size distribution, as it is shown in Figure 5.

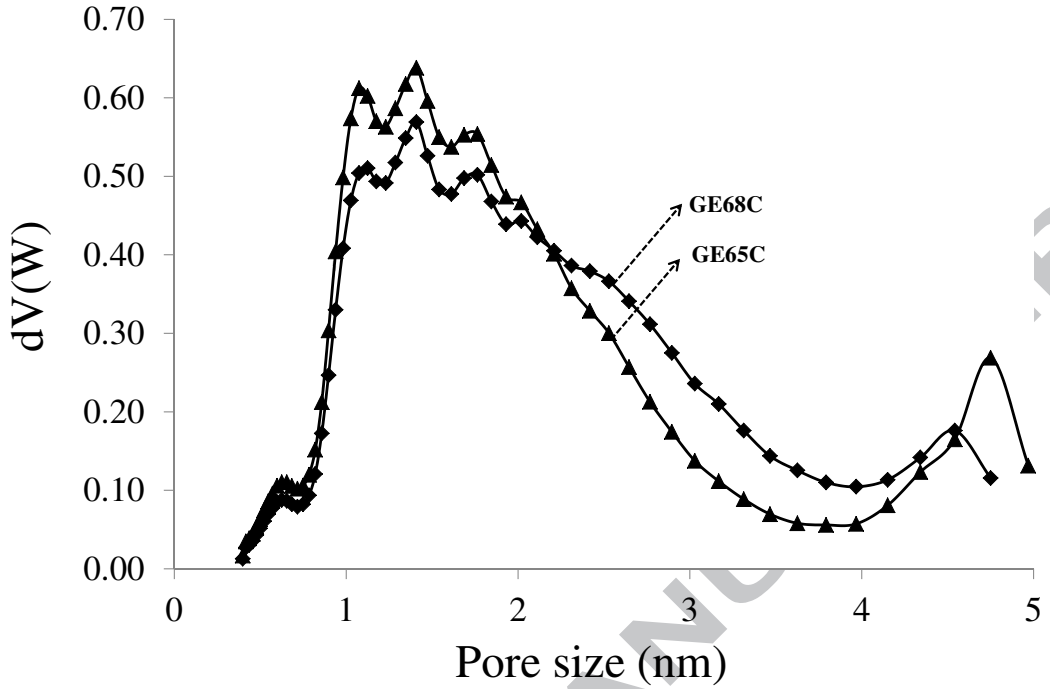

Fig. 5. Effect of the CO_2 activation rate on the resulting pore size distributions of GE65C and GE68C (calculated applying the NLDFT model to the N_2 adsorption data at -196 ºC)

3.5. Toluene adsorption

Several samples have been selected for toluene adsorption experiments; the pristine precursor, the two commercial samples, and five SACs. These selected SACs include samples that have been prepared with both activating agents, have different properties and have been prepared using similar activation rates (GE60C and GE57S) or different activation rates (GE65C and GE65S). Figure 6 shows, as an example, the breakthrough curves of three samples (GE, WVA1100 and GE65S). Similar curves have been obtained for the other samples. The breakthrough curves of all the studied samples have been used to calculate their adsorption capacities by numerical integration of their areas. Table 3 compiles the total oxygen contents of the samples (determined from the amounts of CO_2 and CO evolved from TPD runs) and their toluene adsorption

capacities, expressed both per gram of sample and per bed volume (using the samples densities).

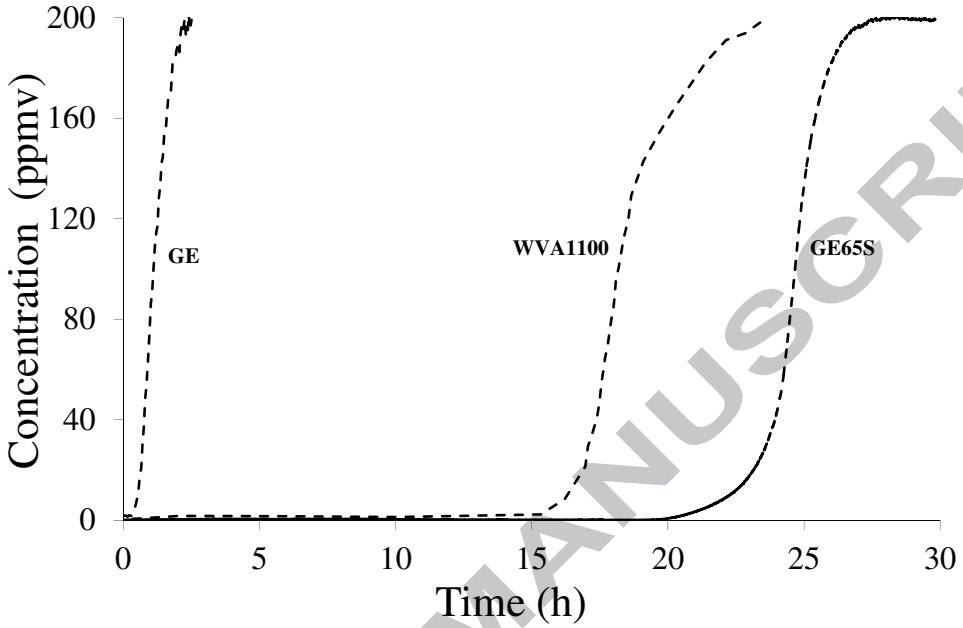

Fig. 6. Breakthrough curves for toluene adsorption plotted versus time on three samples used as examples.

In relation to the oxygen contents, it can be observed that: i) most of the SACs have low surface oxygen contents, many of them even lower than pristine GE, especially those activated with CO_2, ii) steam produces higher surface oxygen contents than CO_2, iii) two of the samples with highest oxygen contents are the two commercial samples and iv) toluene adsorption results are not influenced by the oxygen surface contents.

As expected, toluene adsorption capacities increase with the degree of activation of the samples, varying from 31 to 46 g toluene/100 g AC, or in a volumetric basis from 90 to 236 g toluene/L AC. These values are much larger than those achieved with the

carbonized GE precursor (3 g toluene/100 g or 26 g toluene/L GE), as it is shown in Table 3.

It must also be remarked that, after exhaustion, these samples can be fully regenerated using an helium flow of 90 ml and 400ºC temperature, held for four hours.

Table 3. Total oxygen content, gravimetric and volumetric adsorption capacities for toluene when processing an air stream that contains 200 ppmv toluene.

Sample	Total oxygen content* (µmol/g)	Gravimetric adsorption capacity $\left(\frac{g\ toluene}{100\ g\ AC}\right)$	Volumetric adsorption capacity $\left(\frac{g\ toluene}{l\ AC\ bed\ AC}\right)$	$\left(\frac{V_{toluene}^{**}}{V_{DR}CO_2}\right)$
GE	684	3	26	0.16
GE31C	385	38	236	0.91
GE65C	304	46	179	0.82
GE65S	3015	40	196	0.83
GE57S	1180	40	224	0.94
GE60C	390	46	203	0.92
ACGE	1472	43	198	0.78
WVA1100	2707	31	90	0.97

* Total oxygen content = $CO + 2CO_2$.

** $V_{toluene}$ = Volume of toluene adsorbed as a liquid

Previous papers [1,44,45] have shown that the adsorption at low concentration of benzene or toluene (especially for the former) correlates much better with the narrow micropore volume ($V_{DR}CO_2$) than with the apparent BET surface of the sample studied. Results in Table 3 and Figure 7 confirm these observations. Thus, it can be seen that the toluene gravimetric adsorption capacities of the samples correlate much better with their narrow micropore volumes (Figure 7b) than with their apparent BET surface areas (Figure 7a). In summary, the narrow micropore volume controls the toluene gravimetric adsorption capacity; the highest toluene gravimetric adsorption capacity corresponds to

sample GE65C, which has the highest narrow micropore volume (0.63 cm^3/g), whereas sample WVA1100, having the lowest narrow micropore volume, presents the lowest toluene gravimetric adsorption capacity.

Furthermore, the ratio of the volume of toluene adsorbed as liquid (considering toluene density of 0.862 g/cm^3) to the volume of the narrow micropore (<0.7 nm) for all the samples (except for GE, which is a carbonized material with a poor developed porosity) is in all the cases near 1, especially for similar burn-off percentages (see Table 3). This indicates, and confirms, that toluene is basically adsorbed in these narrow micropores (< 0.7 nm) and fills most of them.

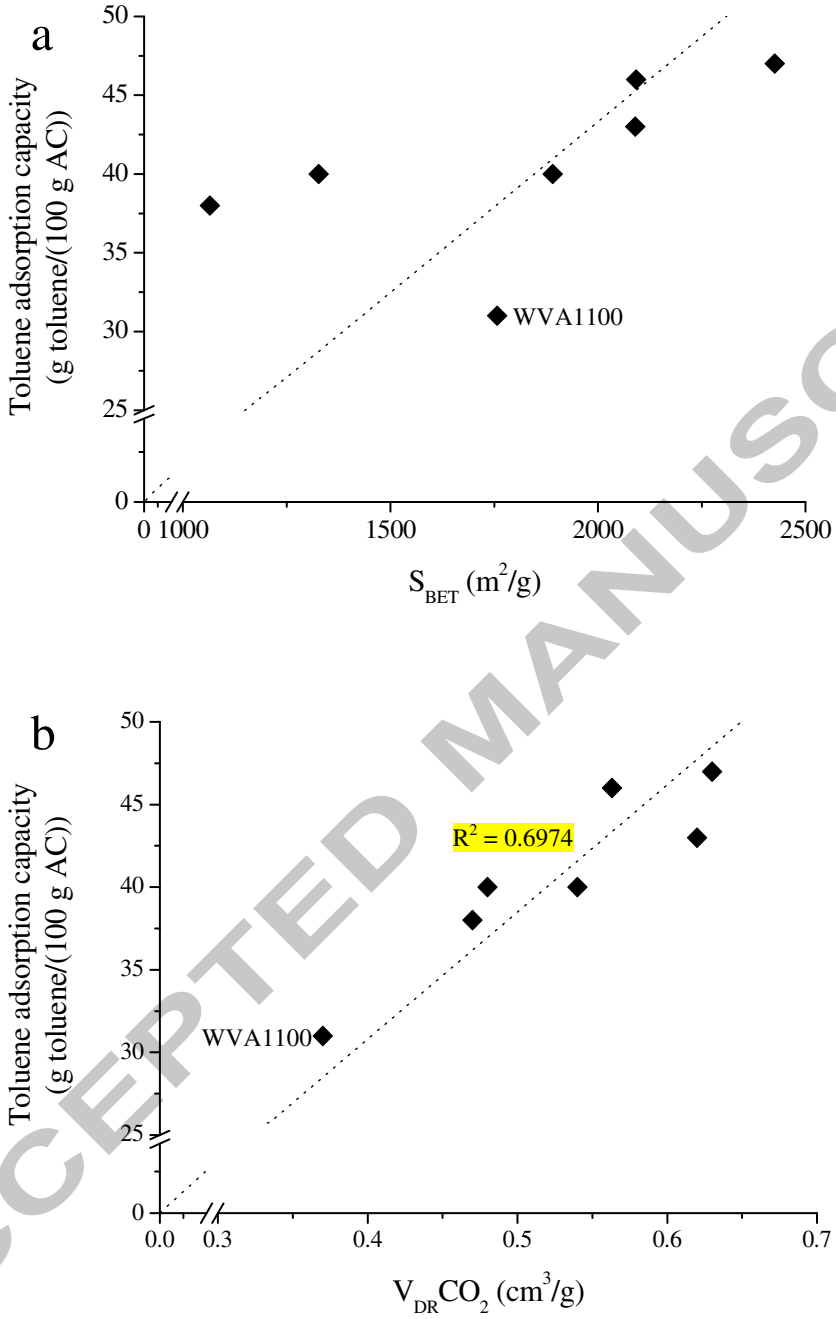

Fig. 7. Toluene gravimetric adsorption capacity vs apparent BET surface area (a) and vs narrow micropore volume (b). In Figure 7b the regression line passes through the origin.

As stated before, the gravimetric adsorption capacities increase (e.g., $V_{DR}CO_2$) with the increase in the burn-off percentage, but the samples bed densities decrease, which will affect the resulting toluene volumetric adsorption capacity of the samples. Thus, in terms of volumetric adsorption capacity, Figure 8a shows that narrow microporosity is not the only parameter affecting the performance of the samples. This plot and data of Tables 1 and 3 permits to observe that samples with low-moderate porosity development present the largest toluene volumetric adsorption capacity. Figure 8b, that presents the volumetric toluene adsorption capacities as a function of the samples densities, allows to confirm the strong influence that the samples bed densities have on the volumetric adsorption capacities.

The performance of sample WVA1100 merits an additional comment. In principle, the data of this sample appears somewhat unexpected; it follows the same trend as the other samples in Figure 7b, but performs considerably different that other samples in Figure 8a and b. This apparent anomaly can be explained considering its different porosity; it has, in addition to microporosity, an important contribution of larger pores (especially mesopores). Consequently, its density, for a comparable micropore volume (Figure 8a and b), is much lower than those for the spherical activated carbons.

Considering all this it can be stated that the combination of both parameters, narrow micropore volume and bed density, determines the toluene volumetric adsorption capacity of the samples, as it can be clearly shown in Figure 8c, where both parameters (micropore volume and bed density) have been considered. Activation leads

to a more pronounced bed density decrease, in comparison with the increase in the narrow micropore volume, therefore being bed density importantly determining volumetric adsorption capacity.

In summary, our results clearly show that samples combining high narrow micropore volume and, especially, high bed density maximize volumetric toluene adsorption at low concentration. Thus, the best SAC sample studied in this work from the point of view of its volumetric adsorption capacity (236 g toluene/L) is GE31C, which has S_{BET} of 1065 m^2/g, $V_{DR}CO_2$ of 0.47 cm^3/g and bed density of 0.62 g/cm^3. This volumetric adsorption capacity value is somewhat higher than the best one prepared from the activation of a commercial SAC, which was 230 g toluene/L and corresponded to a sample having S_{BET} = 1291 m^2/g, $V_{DR}CO_2$ =0.42 cm^3/g, and bed density of 0.59 g/cm^3 [1].

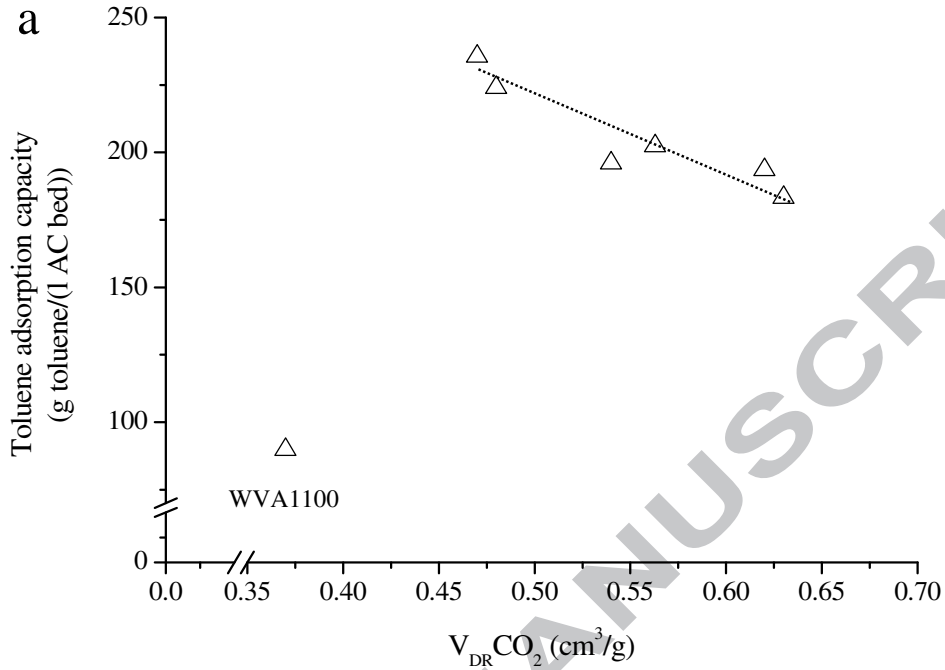

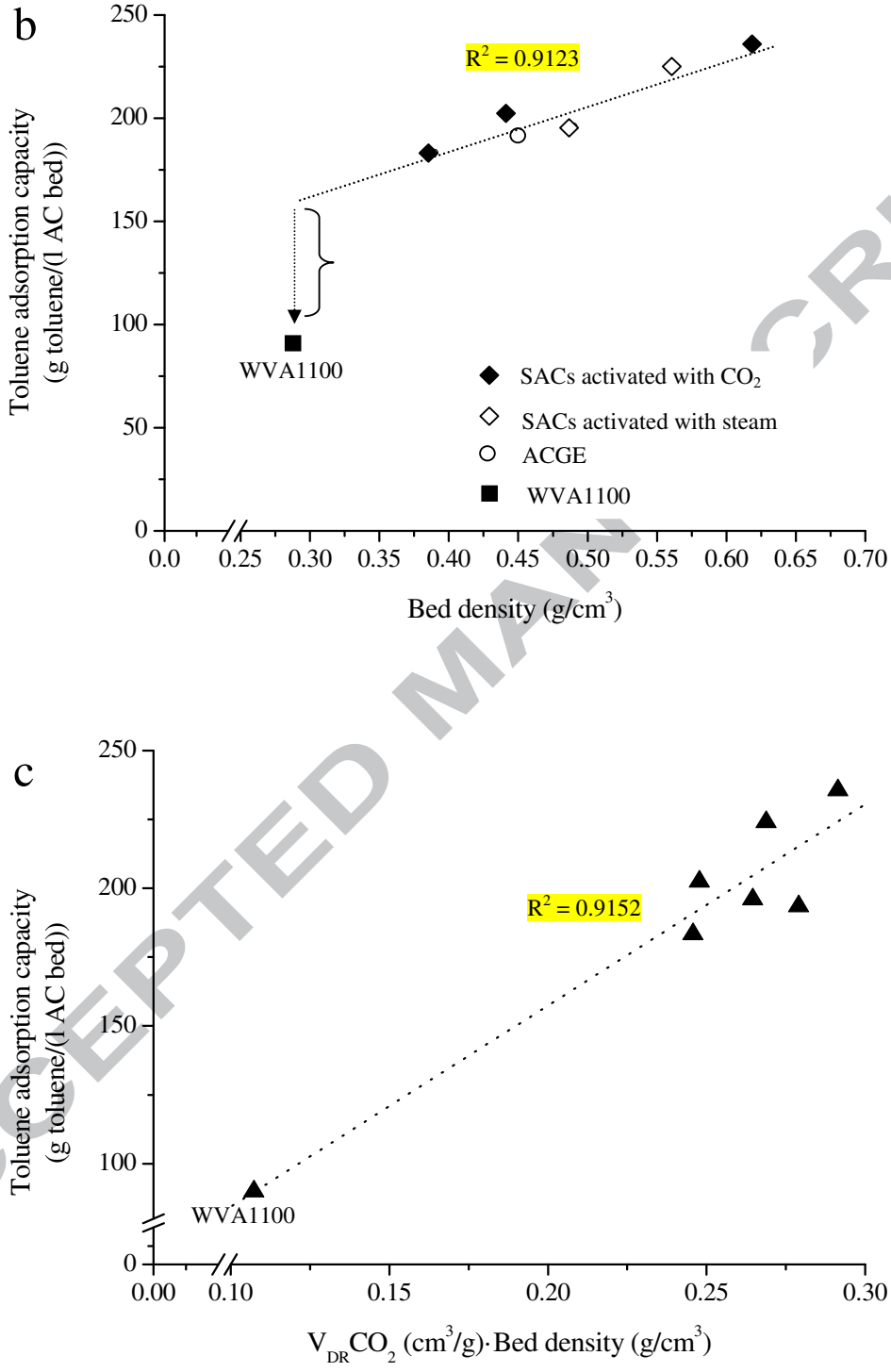

Fig. 8. Toluene volumetric adsorption capacity vs narrow micropore volume (a), vs bed density, (b), and versus the product narrow micropore volume·bed density (c). In Figure

8b R^2 regression was calculated avoiding WVA1100 sample and regression line does not pass through the origin. In Figure 8c the regression line passes through the origin.

4. Conclusions

From a selected high density and low porosity commercial spherical carbon a series of spherical activated carbons have been prepared. Two activating agents (steam and CO_2) have been used and compared using similar and/or different activation rates and keeping comparable the burn-off percentages. The selected spherical carbon can be well activated with by both activating agents although their porosity developments differ. Thus, for a similar burn-off percentage, CO_2 activation leads to larger porosity developments, penetrates more inside the spherical particles and hence produces a lower mean particle size reduction than steam activation which steam activates more from the outside to the interior of the spheres. For a comparable burn-off percentage, steam allows to prepare samples with higher densities but with lower porosities than CO_2.

The activation rate has been analysed using two different rates and the activation results have been compared (CO_2 vs CO_2 and steam vs CO_2). The activation rate affects the pore size distribution (higher rate produces wider pore size distribution) but neither the porosity development, nor the sample density.

The importance of the narrow microporosity and bed density on toluene adsorption capacity at low pressure has been confirmed. Thus, in general an increase in the burn-off percentage leads to a porosity development, which is beneficial for toluene adsorption capacity. However, bed density lowers as a result of the activation, what is detrimental for toluene volumetric adsorption capacity, and therefore for optimizing

volumetric adsorption capacity both parameters, porosity and bed density of the adsorbent, have to be taken into account.

The prepared SACs have suitable characteristics for toluene adsorption at low concentrations; they have both high microporosity and high bed density. Spherical activated carbons with high adsorption gravimetric capacity have been prepared, leading to adsorption capacities as high as 38 g toluene/100g for GE31C and 46 g toluene/100g for GE60C. From the point of view of the volumetric adsorption capacity, it should be highlighted that the obtained values are quite high, especially for the GE31C sample (236 g of toluene/L), and that a combination of a narrow micropore volume and a large bed density is desirable.

Acknowledgements

The authors thank Generalitat Valenciana (Prometeo/2009/047 and FEDER), MICINN and plan E (CTQ2012-3176) and MINECO (MAT-2012-32832) for financial support.

References

[1] Romero-Anaya AJ, Lillo-Ródenas MA, Linares-Solano A. Spherical activated carbons for low concentration toluene adsorption. Carbon 2010;48:2625-33.

[2] Anastas PT, Warner JC, Green Chemistry. Theory and Practice, Oxford University Press, New York: 1998.

[3] Cal MP, Larson SM, Rood MJ. Experimental and Modeled Results Describing the adsorption of acetone and benzene onto activated carbon fibers. Environ. Progress 1994;13:26-30.

[4] Wu CF, Wu SY, Wu YH, Cullen AC, Larson TV, Williamson J, et al. Cancer risk assessment of selected hazardous air pollutants in Seattle. Environ. Int. 2009;35:516–22.

[5] Dolidovic AF, Akhremkova GS, Efremtsev WS. Novel Technologies of VOC Decontamination in Fixed, Moving and Fluidized Catalyst-Adsorbent Beds. The Can. J. of Chem. Eng 1999;77:342-55.

[6] Fletcher AJ, Yüzak Y, Thomas KM. Adsorption and desorption kinetics for hydrophilic and hydrophobic vapors on activated carbon. Carbon 2006;44:989-1004.

[7] Yun JH, Hwang KY, Choi DK. Adsorption of Benzene and Toluene Vapors on Activated Carbon Fiber at 298, 323, and 348 K. J. Chem. Eng. Data 1998; 43:843-45.

[8] Ghoshal AK, Manjare SD. Selection of appropriate adsorption technique for recovery of VOCs: an analisys. J. of Loss Prev. in the Process. Ind 2002;15:413-21.

[9] Khan FI, Ghoshal AK. Removal of Volatile Organic Compounds from polluted air. J. of Loss Prev. in the Process. Ind. 2000;13:527-45.

[10] Lillo-Ródenas MA, Carratalá-Abril J, Cazorla-Amorós D, Linares-Solano A. Usefulness of chemically activated anthracite for the abatement of VOC at low concentrations. Fuel Process. Technol 2002;77-78:331-6.

[11] Van De Beld L, Bijl MPG, Reinders A, Van Der Werf B, Westerterp KR. The catalytic oxidation of organic contaminants in a packed bed reactor. Chem. Eng. Sci. 1994;49:4361-73.

[12] Bouazza N, Lillo-Ródenas MA, Linares-Solano A. Photocatalytic activity of TiO_2-based materials for the oxidation of propene and benzene at low concentration in presence of humidity. Appl. Catal B: Environ. 2008;84:691-8.

[13] Hort C, Gracy S, Platel V, Moynault L. Evaluation of sewage sludge and yard waste compost as a biofilter media for the removal of ammonia and volatile organic sulfur compounds (VOSCs). Chem. Eng. J. 2009;152:44-53.

[14] Sing Kenneth SW. Adsorption by powders and porous solids. (Second Edition). Principles, methodology and applications, 2014, Pages 321-391.

[15] Lillo-Ródenas MA, Fletcher AJ, Thomas KM, Cazorla-Amorós D, Linares-Solano A. Competitive adsorption of a benzene–toluene mixture on activated carbons at low concentration. Carbon 2006;44:1455-63.

[16] Carratalá-Abril J, Lillo-Ródenas MA, Linares-Solano A, Cazorla-Amorós D. Activated Carbons for the Removal of Low-Concentration Gaseous Toluene at the Semipilot Scale, Ind. Eng. Chem. Res 2009;48:2066-75.

[17] Liu Z, Ling L, Qiao W, Liu L. Effect of hydrogen on the mesopore development of pitchbased spherical activated carbon containing iron during activation by steam. Carbon 1999;37:2063-66.

[18] Wang Q, Liang XY, Zhang R, Liu CJ, Liu XJ, Qiao WM, et al. Preparation of polystyrene-based activated carbon spheres and their adsorption of dibenzothiophene. New Carbon Materials 2009;24:55-60.

[19] Lee CJ, Hsu ST. Preparation of spherical encapsulation of activated carbons and their adsorption capacity of typical uremic toxins. J Biomed Mater Res. 1990;24:243–58.

[20] Böhringer B, Guerra Gonzalez O, Eckle I, Müller M, Giebelhausen JM, Schrage C, et al. Polymer-based Spherical Activated Carbons -From Adsorptive Properties to Filter Performance. Chemie Ingenieur Technik 2011;83:53-60.

[21] Liu C, Liang X, Liu X, Wang Q, Teng N, Zhan L, et al. Wettability modification of pitch-based spherical activated carbon by air oxidation and its effects on phenol adsorption. Applied Surface Science 2008;254:2659-65.

[22] Long D, Zhang R, Qiao W, Zhang L, Liang X, Ling L. Biomolecular adsorption behavior on spherical carbon aerogels with various mesopore sizes. Journal of Colloid and Interface Science 2090;331:40–6.

[23] Zhu Z, Li A, Yan L, Liu F, Zhang Q. Preparation and characterization of highly mesoporous spherical activated carbons from divinylbenzene-derived polymer by $ZnCl_2$ activation. J Colloid Interface Sci.2007;316:628-34.

[24] Wang D, Chen M, Wang C, Bai J, Zheng J. Synthesis of carbon microspheres from urea formaldehyde resin. Materials Letters. 2011;65:1069-72.

[25] Gryglewicz G, Grabas K, Lorenc-Grabowska E. Preparation and characterization of spherical activated carbons from oil agglomerated bituminous coals for removing organic impurities from water. Carbon 2000;40:2403-11.

[26] Oh WC, Kim JG, Kim H, Chen ML, Zhang FJ, Zhang K, et al. Preparation of Spherical Activated Carbon and Their Physicochemical Properties. Journal of the Korean Ceramic Society 2009;46:568-73.

[27] Luo G, Shi W, Chen X, Ni W, Strong PJ, Jia Y, et al. Hydrothermal conversion of water lettuce biomass at 473 or 523 K. Biomass and Bioenergy 2011;35:4855-61.

[28] Hoekman SK, Broch A, Robbins C. Hydrothermal Carbonization (HTC) of Lignocellulosic Biomass. Energy Fuels 2011;25:1802-10.

[29] Sevilla M, Maciá-Agulló JA, Fuertes AB. Hydrothermal carbonization of biomass as a route for the sequestration of CO_2: Chemical and structural properties of the carbonized products. Biomass and Bioenergy 2011;35:3152-9.

[30] Sun X, Li Y. Ga_2O_3 and GaN semiconductor hollow spheres. Angew Chem Int Ed Engl. 2004;43:3827-31.

[31] Yao C, Shin Y, Wang LQ, Windisch CF, Samuels WD, Arey BW, et al. Hydrothermal Dehydration of Aqueous Fructose Solutions in a Closed System. J. Phys. Chem. C 2007;111:15141-45.

[32] Sevilla M, Fuertes AB. The production of carbon materials by hydrothermal carbonization of cellulose. Carbon 2009;47:2281-9.

[33] Wang FL, Pang LL, Jiang YY, Chen B, Lin D, Lun N, et al. Simple synthesis of hollow carbon spheres from glucose. Materials Letters 2009;63:2564-6.

[34] Linares-Solano A, Salinas-Martínez de Lecea C, Alcañiz-Monge J, Cazorla-Amorós D. Further advances in the characterization of microporous carbons by physical adsorption of gases. Tanso 1998;185:316–25.

[35] Cazorla-Amorós D, Alcañiz-Monge J, Linares-Solano A. Characterization of activated carbon fibers by CO_2 adsorption. Langmuir 1996;12:2820–4.

[36] Rodríguez-Reinoso F, Linares Solano A. Microporous structure of activated carbons as revealed by adsorption methods. In: Thrower PA, editor. Chemistry and physics of carbon, vol 21. New York: Marcel Dekker; 1988. p. 1-146.

[37] Lozano-Castelló D, Cazorla-Amorós D, Linares-Solano A. Usefulness of CO_2 adsorption at 273 K for the characterization of porous carbons. Carbon 2004;1231-1236.

[38] Jagiello J, Thommes M. Comparison of DFT characterization methods based on N_2, Ar, CO_2, and H_2 adsorption applied to carbons with various pore size distributions. Carbon 2004;42:1227-32.

[39] Román-Martínez MC, Cazorla-Amorós D, Linares-Solano A, Salinas-Martínez de Lecea C. TPD and TPR characterization of carbonaceous supports and Pt/C catalysts. Carbon 1993;31:895-902.

[40] Rouquerol F, Rouquerol J, Sing K. Adsorption by powders and porous solids. Principles, methodology and applications. London: Academic Press; 1999.

[41] Baghel A, Singh B, Prasad GK, Pandey P, Gutch PK. Preparation and characterization of active carbon spheres prepared by chemical activation. Carbon 2011;49:4739-44.

[42] Tennison SR. Phenolic-resin-derived activated carbons. Applied Catalysis A: General 1998;13:289-311.

[43] Alcañiz-Monge J, Cazorla-Amorós D, Linares-Solano A, Yoshida S, Oya A. Effect of the activating gas on tensile strength and pore structure of pitch-based carbon fibres. Carbon 1994;32:1277-83.

[44] Lillo-Ródenas MA, Cazorla-Amorós D, Linares-Solano A. Behaviour of activated carbons with different pore size distributions and surface oxygen

groups for benzene and toluene adsorption at low concentrations. Carbon 2005;43:1758-67.

[45] Lillo-Ródenas·MA, Cazorla-Amorós D, Linares-Solano A. Benzene and toluene adsorption at low concentration on activated carbon fibres. Adsorption 2010;17:473-81.